

Design and Implementation of a 4x2 Diamond Patch Array Microstrip Antenna with I-Slot for 2.4 GHz Frequency

Ade Dwi Arya¹, Koesmariyanto Koesmariyanto^{2*}, Hudiono Hudiono³

^{1,3} Digital Telecommunication Network Study Program, Department of Electrical Engineering, State Polytechnic of Malang, 65141 Indonesia

² Telecommunication Engineering Study Program, Department of Electrical Engineering, State Polytechnic of Malang, 65141 Indonesia

¹adedwiarya@gmail.com, ²koesmariyanto@polinema.ac.id, ³hudiono@polinema.ac.id

Abstract— As communication technology continues to evolve rapidly, particularly in the field of wireless communication, there is a growing demand for high-speed, efficient, and high-quality communication systems due to the increasing mobility of society. Microstrip antennas offer the advantages of being small, inexpensive, and lightweight. However, these antennas typically have low gain and bandwidth. Various methods have been proposed to enhance the gain of microstrip antennas, such as the addition of slots to the patch. This research presents an external device, a microstrip antenna, that can increase data transfer capacity and operates at the Wi-Fi frequency of 2.4 GHz. The fabricated 4x2 I-Slot Diamond Patch Array Microstrip Antenna demonstrates improved performance with a measured return loss of -17.3 dB and VSWR of 1.3 at 2.4 GHz. The incorporation of the I-slot and array configuration results in a bandwidth of 105 MHz, which is 9 MHz wider compared to a similar antenna without the slot (96 MHz). In outdoor range testing, the proposed antenna achieves a maximum communication distance of 30 meters with an RSSI of -72 dBm, outperforming the built-in antenna which yields -77 dBm at the same distance.

Keywords— Array, Bandwidth Enhancement, Diamond Patch Antenna, I-Slot Antenna, Microstrip Patch Antenna, Wi-Fi Antenna.

I. INTRODUCTION

The proliferation of the Internet of Things (IoT), smart devices, and high-density wireless local area networks (WLANs) has exponentially increased the demand for robust and efficient wireless communication systems operating in the unlicensed 2.4 GHz Industrial, Scientific, and Medical (ISM) band [1], [2]. As a critical interface in these systems, antennas are required to exhibit enhanced performance metrics, including improved gain, wider bandwidth, and stable radiation patterns, to support high data-rate applications and mitigate interference in congested spectral environments [3], [4].

Microstrip patch antennas are a predominant choice for modern compact wireless devices due to their low profile, light weight, ease of fabrication, and conformability to planar structures [5], [6]. However, conventional single-element microstrip antennas suffer from inherent limitations, notably narrow impedance bandwidth and moderate gain, which constrain their efficacy in contemporary wideband and long-range applications [7], [8]. To overcome these constraints, extensive research has focused on various performance enhancement techniques. Employing an array configuration is a well-established method to significantly boost gain and directivity by coherently combining the radiation from multiple patch elements [9], [10].

Concurrently, the integration of slot geometries into the radiating patch has emerged as a highly effective technique for impedance bandwidth broadening. Slots perturb the surface current distribution, introduce additional resonant modes, and can facilitate improved impedance matching over a wider

frequency range [11], [12]. Among various slot shapes, I-shaped slots have been demonstrated to effectively create multi-resonance behavior, leading to substantial bandwidth enhancement while maintaining a compact antenna footprint [13], [14]. Furthermore, the shape of the fundamental radiating patch itself is a critical design parameter. Diamond-shaped patches, compared to traditional rectangles, offer a larger effective radiating perimeter for a given occupied area, which can contribute to better radiation efficiency and broader bandwidth [15], [16].

Recent investigations have explored the synergistic combination of these techniques. Studies on array configurations with modified patch shapes (e.g., hexagonal, octagonal) and different slot types (U-slot, H-slot, T-slot) for 2.4 GHz applications have reported promising results in gain and bandwidth improvement [17], [18]. However, a comprehensive analysis of a high-gain array architecture utilizing a diamond-shaped patch element integrated with a complementary I-slot remains underexplored in the recent literature. This specific combination leverages the geometrical advantages of the diamond patch for efficiency alongside the resonant-tuning capability of the I-slot for bandwidth extension, all within a scalable array topology.

This research, therefore, presents the design, simulation, fabrication, and measurement of a 4x2 Diamond Patch Array Microstrip Antenna with an I-Slot for operation at 2.4 GHz. The primary objective is to synthesize an antenna that surpasses the performance of standard patches by achieving superior gain and enhanced bandwidth simultaneously. The

*Corresponding author

design methodology encompasses full-wave electromagnetic simulation for optimization, followed by experimental validation. Key performance parameters, including return loss, voltage standing wave ratio (VSWR), impedance bandwidth, radiation pattern, and gain, are rigorously characterized and compared against conventional designs. The proposed antenna is intended to serve as a high-performance component for advanced Wi-Fi routers, IoT gateways, and other wireless communication systems requiring reliable links in the 2.4 GHz band.

II. METHOD

The design that will be used in the research is the creation of stages of information search, tool manufacturing to testing, in a thesis that is prepared with the intention that the research is carried out in detail and planned through the stages that have design.

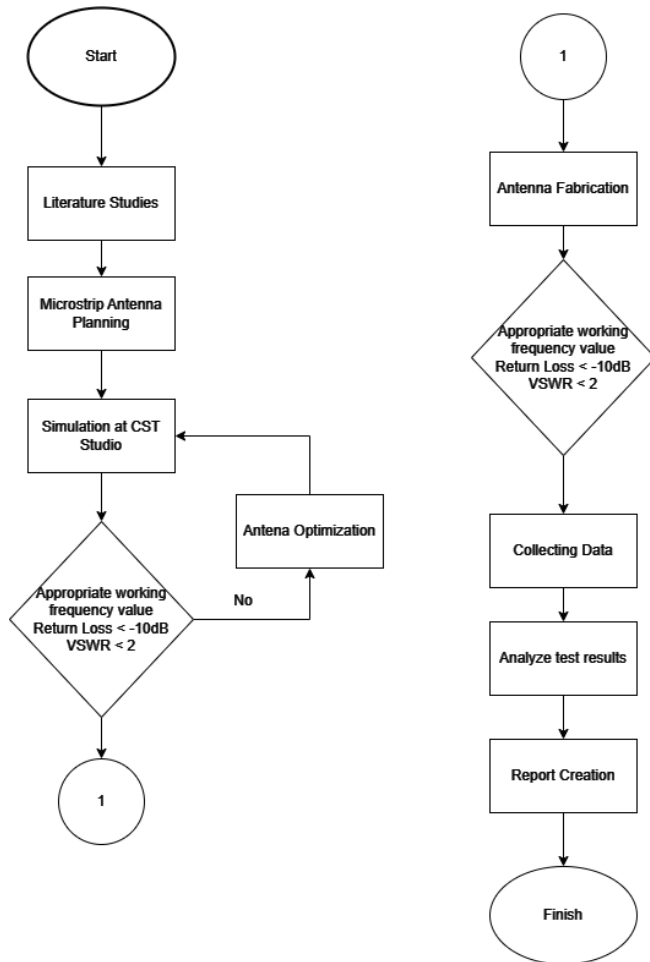


Figure 1. Research flow chart

A. Antenna Design

1) *Element Patch Design*: The planned diamond-shaped antenna has a 2448MHz transceiver resonance with a slot in the diamond patch. Calculating Rectangular Width with formula (1).

$$W_p = \frac{c}{2 \times f_r} \times \sqrt{\frac{2}{\epsilon_r + 1}} \quad (1)$$

Information:

W_p = Wide Patch

f_r = Working Frequency (Hz)

ϵ_r = Dielectric Constant

The width of the rectangular antenna patch was 36.66mm. Then find the length of the rectangular patch with the formula (2).

$$L_p = \frac{c}{2 \times f_r \times \sqrt{\epsilon_{eff}}} - 2\Delta_L \quad (2)$$

Information:

L_p = Patch Length

c = speed of lights (m/s)

f_r = Working Frequency (Hz)

The Length of the rectangular antenna patch was 28,24mm.

From the results above, the length and width of the rectangular antenna patch are obtained. To calculate the length of the diagonal side of a rectangular antenna into a diamond antenna with the formula (3).

$$x = \sqrt{\left(\frac{L_p}{2}\right)^2 + \left(\frac{W_p}{2}\right)^2} \quad (3)$$

Information:

L_p = Patch Length

W_p = Patch Width

X = Diagonal Side Length

From the results above, the side length is 23.13mm. then to find the length and width of the I-Slot requires the formula (4).

$$\begin{aligned} C &= \frac{\lambda_0}{60} \\ E &= 0,3x X \end{aligned} \quad (4)$$

Information:

C = Slot Width

E = Slot Length

From the calculation above, the slot length is 6.93mm and the width is 2.04mm.

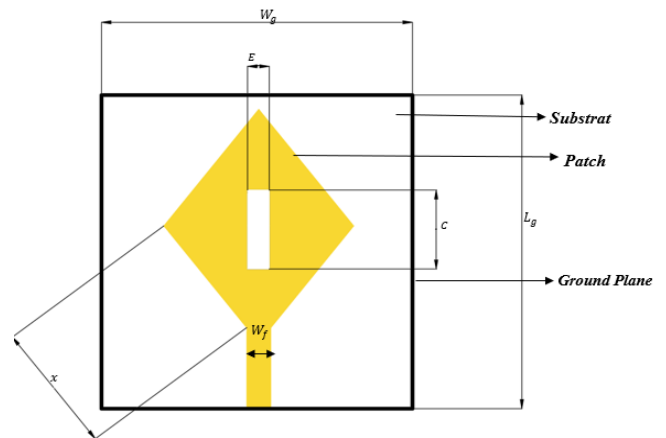


Figure 2. Diamond patch antenna with i-slot

2) *Transmission Line Design*: The impedance and transmission line specifications for the system are as follows: The impedance of the supply, denoted as Z_6 , is measured at 50 Ohms, while the impedance of the channel, denoted as Z_{in} , is 150 Ohms. These impedance values are essential for maintaining proper signal integrity and minimizing reflection losses in the system.

In addition to the impedance, the transmission line widths are carefully specified for optimal performance across different sections. Wf1 is 1.65 mm, providing a narrow path for precise signal transmission. Wf2, slightly wider at 3.2 mm, meets varying frequency needs. Wf3 is significantly larger at 74 mm, likely for high-power transmission or broader bandwidths. Wf4 measures 16.53 mm, Wf5 is 29.4 mm, Wf6 is 12.8 mm, and Wf7 is 7.4 mm, each tailored for specific signal characteristics and system requirements.

These dimensions are critical for achieving the desired electrical performance, minimizing loss, and ensuring that the transmission line operates efficiently across its entire length.

3) *Designing the length of the transmission line*: The lengths of the transmission line components are designed as follows: The total length of the transmission line, denoted as LT, is 14.315 mm. The individual section lengths are specified as follows: Lf1 is 8.18 mm, Lf2 is 45 mm, Lf3 is 25 mm, Lf4 is 118 mm, Lf5 is 20 mm, Lf6 is 14.3 mm, and Lf7 is 35 mm. These precise measurements are critical for ensuring the transmission line's proper functionality and performance. as shown at Fig. 3.

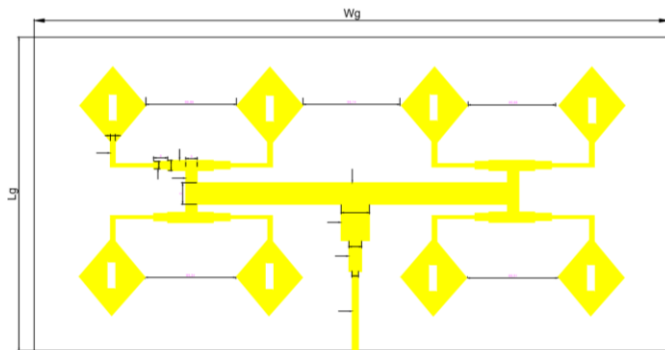


Figure 3. 4x2 Diamond patch antenna with i-slot

B. Implementation of System Design

The system design of the Diamond Array I-Slot 4x2 Patch Microstrip Array Antenna For 2.4 GHz Frequency is in Fig. 4.

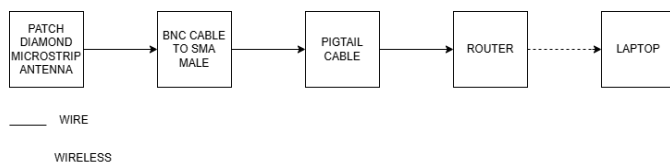


Figure 4. System design implementation design

C. Determination of Material Specifications

The following are the specifications of the materials used in this study. The specifications for the PCB made from FR-4

material are as follows: It features 2 layers (double-sided), with a copper thickness of 0.035 mm. The substrate thickness is 1.57 mm, and the overall size of the PCB is 270 x 160 mm. These specifications ensure durability and optimal performance in the designed application as shown at Table I.

TABLE I
SPECIFICATION PCB FR-4

Details	Specification
Layer	2 (Double)
Copper Thickness	0.035 mm
Substrate Thickness	1.57 mm
Size	270 x 160 mm

III. RESULTS AND DISCUSSION

A. Fabrication Results

The following is the result of fabricating a 4x2 diamond patch microstrip antenna with I-Slot in Fig. 5.



Figure 5. Fabrication results of diamond patch microstrip antenna i-slot array 4x2

B. Return Loss Test Result (Simulation Result)

Fig. 6 Return loss simulation results of a 4x2 diamond patch microstrip antenna with I-Slot.

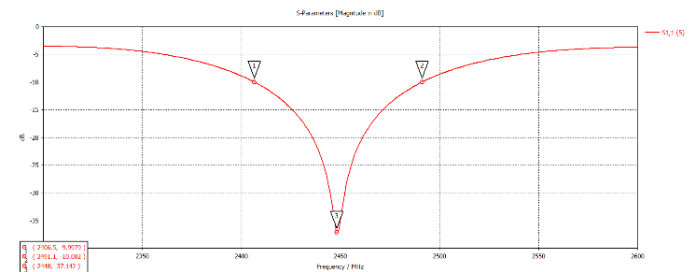


Figure 6. Return loss simulation diamond i-slot array microstrip antenna 4x2

The results of the simulated return loss are -10dB at the frequency of 2406MHz and -10.08dB at the frequency of 2489MHz.

C. VSWR Test Results (Simulation Results)

Fig. 7 VSWR simulation results from a 4x2 diamond patch microstrip antenna with I-Slot.

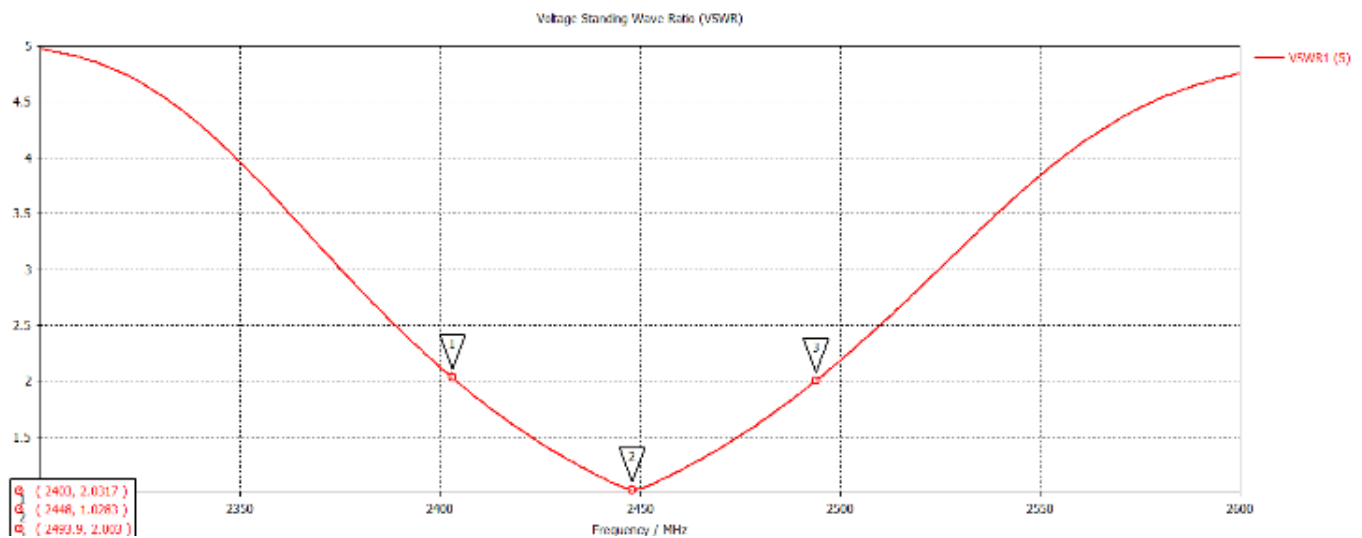


Figure 7. VSWR simulation diamond i-slot array 4x2 microstrip antenna

The results of the simulated VSWR are 2.03 at the frequency of 2406MHz and 2.03 at the frequency of 2489. The frequency of 2448 has a VSWR of 1.02.

D. Bandwidth Test Results (Simulation Results)

Fig. 8 VSWR simulation results from a 4x2 diamond patch microstrip antenna with I-Slot.

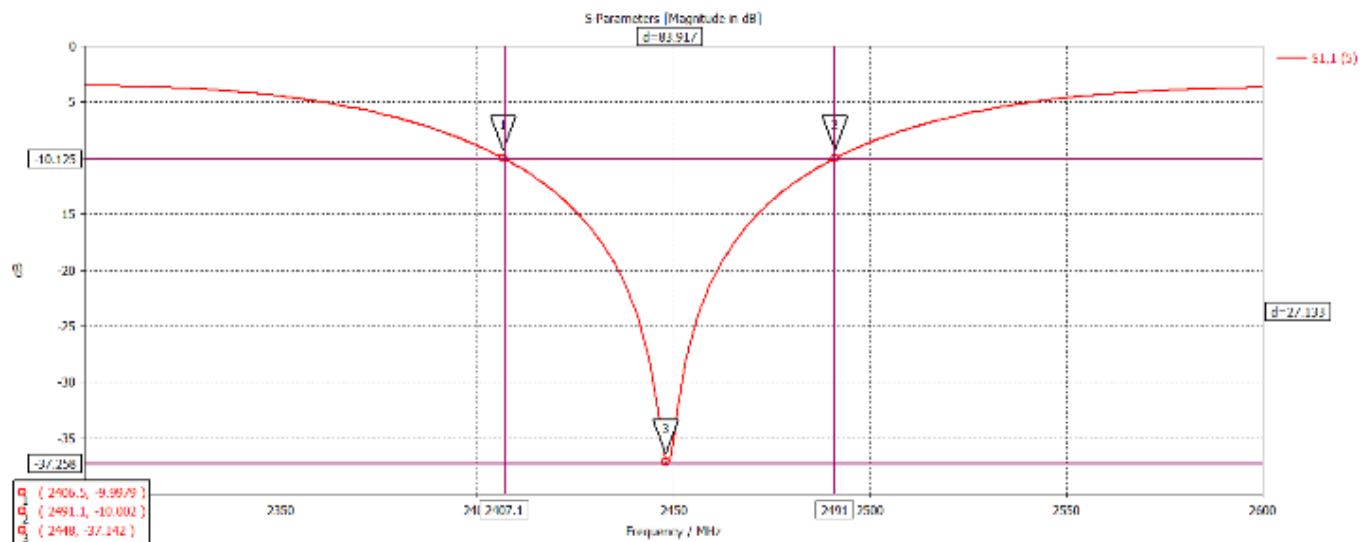


Figure 8. Bandwidth simulation diamond i-slot array 4x2 microstrip antenna

The Bandwidth result of the Antenna is 84Mhz where the upper frequency is 2406MHz and the lower frequency is 2491MHz.

E. Return Loss Test Results

Return loss test results of a 4x2 diamond patch microstrip antenna with I-Slot as shown at Fig. 9.

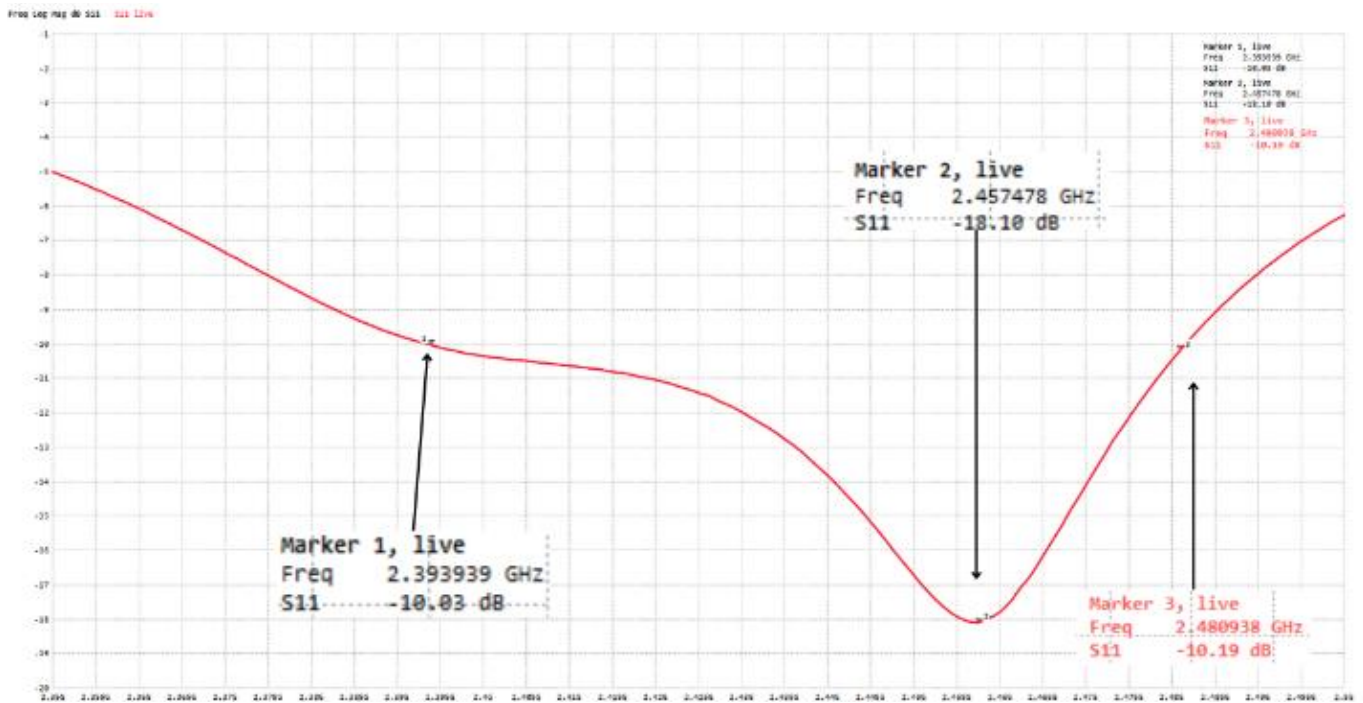


Figure 9. Diamond i-slot array 4x2 microstrip return loss antenna

The return loss test results are -10.03dB at the frequency of 2393MHz and -10.19dB at the frequency of 2480MHz. The frequency of 2457 has the lowest return loss of -18.10dB.

F. VSWR Test Result

Fig. 10 VSWR test results of a 4x2 diamond patch microstrip antenna with I-Slot, VSWR results of the test are 1.9 at the frequency of 2393MHz and 1.89 at the frequency of 2480. The frequency of 2457 has a VSWR of 1.28.

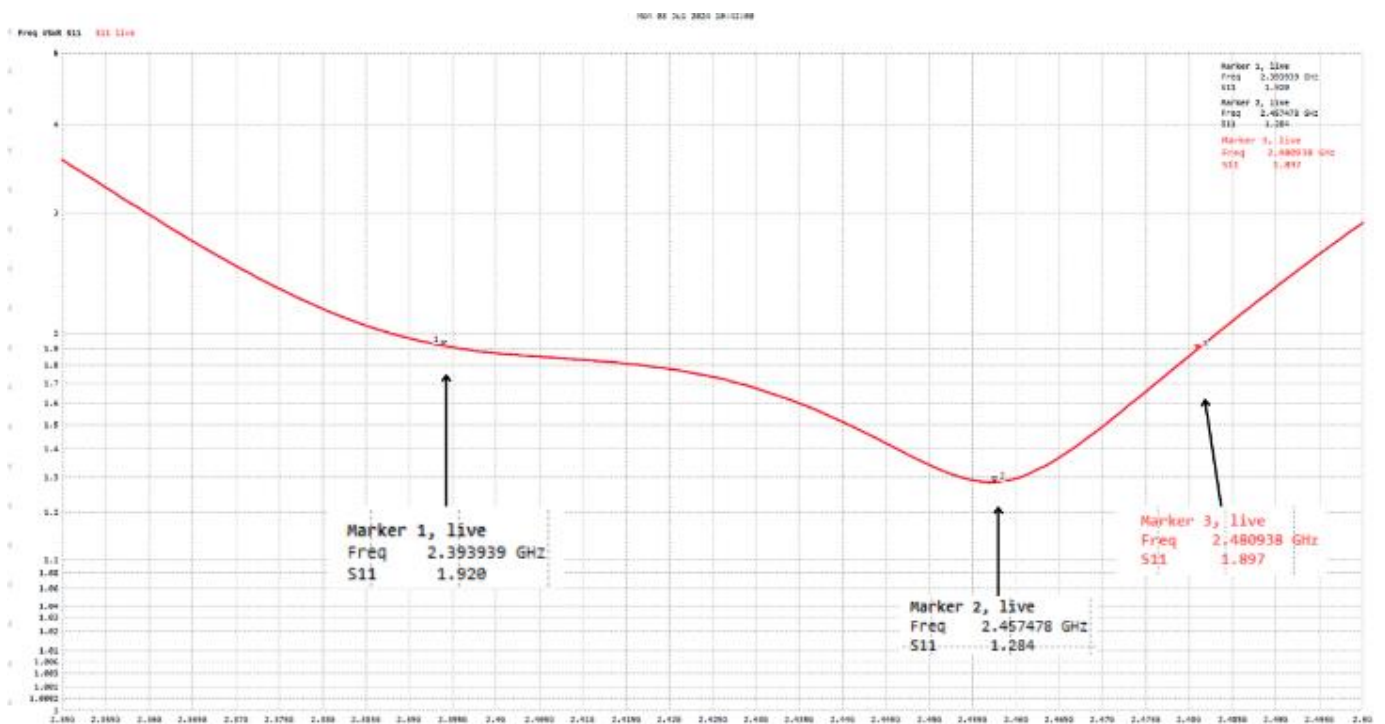


Figure 10. VSWR testing of 4x2 diamond i-slot array microstrip antenna

G. Gain Test Result

Table II gain test results on 4x2 I-Slot diamond patch microstrip antenna.

TABLE II
GAIN TESTING

Frequency (MHz)	Level (dBm)		Gain (dB)
	Antenna Reference	Antena Under Test	
2350	-67.3	-76.1	-6.65
2360	-70.2	-76	-3.65
2370	-68.2	-76.2	-5.85
2380	-74.2	-77	-0.65
2390	-70.3	-74.7	-2.25
2400	-66.3	-72.1	-3.65
2410	-69.7	-68.3	3.55
2420	-73.2	-72.4	2.95
2430	-71.7	-68.2	5.65
2440	-73.5	-67.5	8.15
2450	-64.3	-69.7	-3.25
2460	-64.9	-72.5	-0.45
2470	-62.8	-69.8	-4.85
2480	-63.1	-69.9	-4.65
2490	-63.4	-71	-5.45
2500	-71.7	-71.6	2.25
2510	-66.7	-72.3	-3.45
2520	-71.4	-72.5	1.05

Fig. 11 shows the gain result of a 4x2 diamond patch array microstrip antenna with I-Slot.

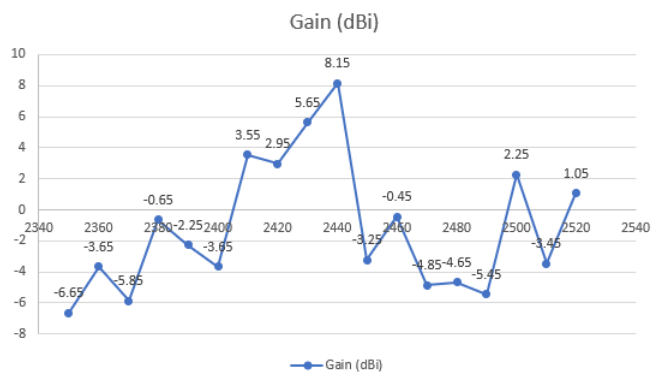


Figure 11. Gain image of diamond microstrip antenna I-slot Array 4x2

From the gain results above, a highest gain result of 8.15dBi was obtained at a frequency of 2440Mhz and the lowest gain result of -6.65dBi at a frequency 2350 Mhz.

H. Radiation Pattern Test Results

Table III Gain test results on 4x2 I-Slot diamond patch microstrip antenna.

TABLE III
RADIATION PATTERN TESTING

Degree Coner	Frequency 2440	
	Power Level (dBm)	Normalization
0°	-66.2	0
10°	-67.4	-1.2
20°	-70.1	-4

30°	-73.2	-7
40°	-74.3	-8.1
50°	-71.7	-5.5
60°	-72	-5.8
70°	-72.5	-6.3
80°	-73.6	-7.4
90°	-77.4	-11.2
100°	-77.7	-11.5
110°	-76.7	-10.5
120°	-75.2	-9
130°	-75.4	-9.2
140°	-76.4	-10.2
150°	-76.9	-10.7
160°	-77.7	-11.5
170°	-78	-11.8
180°	-78.1	-11.9
190°	-77.2	-11
200°	-74.4	-8.2
210°	-76.6	-10.4
220°	-77.1	-10.9
230°	-77.4	-11.2
240°	-77.2	-11
250°	-77.3	-11.1
260°	-77.4	-11.2
270°	-74.4	-8.2
280°	-72.4	-6.2
290°	-71.2	-5
300°	-70.3	-4.1
310°	-70.2	-4
320°	-69.7	-3.5
330°	-68.5	-2.3
340°	-67.1	-0.9
350°	-66.3	-0.1

From the results of the table III, the results of the diagram are described in Fig. 12.

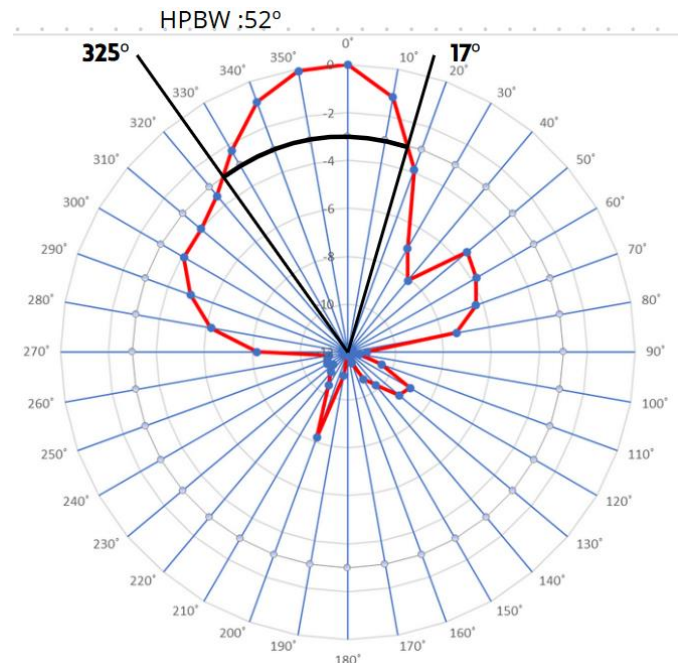


Figure 12. Image of the radiation pattern of the diamond microstrip antenna I-slot array 4x2

The HPBW value can be calculated by marking the normalized value of -3 dB, i.e. HP (left) angle 356° and HP

(right) 3° so that it can be calculated using the following formula:

$$\begin{aligned} HPBW &= HP_{right} - HP_{left} \\ HPBW &= (360^\circ - 325^\circ) + 17^\circ \\ HPBW &= 52^\circ \end{aligned} \quad (5)$$

I. Comparison of Simulation Results with Test Results

Fig. 4 shows the results of the return loss simulation on the diamond I-slot Array 4x2 microstrip antenna at a resonant frequency of 2448 with a result of -37.142 and a VSWR of 1.028. In the results of the fabrication test, the return loss results were obtained at the resonant frequency 2457 with a result of -18.10 and VSWR 1.28.

This is very different from the simulation results and the fabrication results. Where there is a shift in the resonant frequency from 2448MHz to 2457, this occurs due to inaccurate fabrication results.

J. Results Implementation of built-in antenna with 4x2 diamond i-slot array microstrip patch antenna

The implementation of the antenna on 802.11N wireless was carried out at NADA Coffe Jalan Raya Tlogomas No27, Tlogomas, Lowokwaru. The implementation of built-in antennas and external antennas is installed in an open space (outdoor). The 802.11N wireless USB antenna connects directly to the laptop via a USB port. Picture of the implementation of wifi adapter antenna with USB wireless type 802.11N.

In Fig. 13 and Fig. 14 are the results of the test documentation of the implementation of the built-in antenna with a 4x2 diamond i-slot array microstrip antenna. Fig.14 and Fig.15 are the RSSI results of the built-in antenna and the 4x2 diamond I-Slot Array microstrip antenna in the Vistumber software.



Figure 13. Picture of a built-in antenna network on outdoor



Figure 14. 4x2 array of diamond i-slot array patch microstrips for outdoor signal amplifier

#	Active	Mac Address	SSID	Signal	High Signal	RSSI	High RSSI	Channel	Authentication	Encryption	Network Type	Latitude	Longitude
1	Active	08:05:47:20:03	HAZAR ZINA SEPDI	100%	100%	-45 dBm	-37 dBm	1	WPA2/Personal	CCMP	Infrastructure	N 0.000000	E 0.000000
2	Dead	08:02:20:59:04:03	None	0%	0%	-100 dBm	-75 dBm	11	WPA2/Personal	CCMP	Infrastructure	N 0.000000	E 0.000000
3	Dead	08:02:20:59:04:03	None	0%	0%	-100 dBm	-77 dBm	1	WPA2/Personal	CCMP	Infrastructure	N 0.000000	E 0.000000
4	Dead	08:02:20:59:04:03	None	0%	0%	-100 dBm	-45 dBm	1	WPA2/Personal	CCMP	Infrastructure	N 0.000000	E 0.000000
5	Active	A2:FF:0C:74:08:05	EDU2-B47036027	50%	50%	-77 dBm	-45 dBm	3	WPA2/Personal	CCMP	Infrastructure	N 0.000000	E 0.000000
6	Dead	74:EE:24:90:08:9E	Sunmiat USA	0%	0%	-100 dBm	-49 dBm	9	WPA2/Personal	CCMP	Infrastructure	N 0.000000	E 0.000000
7	Dead	0E:70:02:03:15:40	Infra H07 30	0%	0%	-100 dBm	-57 dBm	1	WPA2/Personal	CCMP	Infrastructure	N 0.000000	E 0.000000
8	Dead	50:9F:02:0F:20	None	0%	0%	-100 dBm	-73 dBm	9	Open	None	Infrastructure	N 0.000000	E 0.000000
9	Active	E4:70:59:02:3C:3C	None Nanyang	50%	50%	-74 dBm	-41 dBm	11	WPA2/Personal	CCMP	Infrastructure	N 0.000000	E 0.000000
10	Active	50:9F:02:0F:20	None Nanyang	67%	67%	-74 dBm	-41 dBm	9	WPA2/Personal	CCMP	Infrastructure	N 0.000000	E 0.000000
11	Dead	02:86:37:08:27:74	win 1024	0%	0%	-100 dBm	-43 dBm	1	WPA2/Personal	CCMP	Infrastructure	N 0.000000	E 0.000000
12	Active	08:05:47:20:03	HAZAR ZINA SEPDI	100%	100%	-45 dBm	-37 dBm	1	WPA2/Personal	CCMP	Infrastructure	N 0.000000	E 0.000000
13	Dead	08:05:47:20:03	HAZAR ZINA SEPDI	0%	0%	-100 dBm	-43 dBm	10	WPA2/Personal	CCMP	Infrastructure	N 0.000000	E 0.000000

Figure 15. Results of the implementation of the built-in antenna at a distance of 0 meter

#	Active	Mac Address	SSID	Signal	High Signal	RSSI	High RSSI	Channel	Authentication	Encryption	Network Type	Latitude	Longitude
1	Active	08:05:47:20:03	HAZAR ZINA SEPDI	100%	100%	-45 dBm	-37 dBm	1	WPA2/Personal	CCMP	Infrastructure	N 0.000000	E 0.000000
2	Dead	08:02:20:59:04:03	None	0%	0%	-100 dBm	-75 dBm	11	WPA2/Personal	CCMP	Infrastructure	N 0.000000	E 0.000000
3	Dead	08:02:20:59:04:03	None	0%	0%	-100 dBm	-75 dBm	1	WPA2/Personal	CCMP	Infrastructure	N 0.000000	E 0.000000
4	Dead	08:02:20:59:04:03	None	0%	0%	-100 dBm	-45 dBm	1	WPA2/Personal	CCMP	Infrastructure	N 0.000000	E 0.000000
5	Active	A2:FF:0C:74:08:05	EDU2-B47036027	50%	50%	-77 dBm	-45 dBm	3	WPA2/Personal	CCMP	Infrastructure	N 0.000000	E 0.000000
6	Dead	74:EE:24:90:08:9E	Sunmiat USA	0%	0%	-100 dBm	-49 dBm	9	WPA2/Personal	CCMP	Infrastructure	N 0.000000	E 0.000000
7	Dead	0E:70:02:03:15:40	Infra H07 30	0%	0%	-100 dBm	-57 dBm	1	WPA2/Personal	CCMP	Infrastructure	N 0.000000	E 0.000000
8	Dead	50:9F:02:0F:20	None	0%	0%	-100 dBm	-73 dBm	9	Open	None	Infrastructure	N 0.000000	E 0.000000
9	Active	E4:70:59:02:3C:3C	None Nanyang	67%	67%	-74 dBm	-41 dBm	11	WPA2/Personal	CCMP	Infrastructure	N 0.000000	E 0.000000
10	Active	50:9F:02:0F:20	None Nanyang	67%	67%	-74 dBm	-41 dBm	9	WPA2/Personal	CCMP	Infrastructure	N 0.000000	E 0.000000
11	Dead	02:86:37:08:27:74	win 1024	0%	0%	-100 dBm	-43 dBm	1	WPA2/Personal	CCMP	Infrastructure	N 0.000000	E 0.000000
12	Active	08:05:47:20:03	HAZAR ZINA SEPDI	100%	100%	-45 dBm	-37 dBm	1	WPA2/Personal	CCMP	Infrastructure	N 0.000000	E 0.000000

Figure 16. Results of the implementation of a 4x2 diamond i-slot array microstrip patch antenna at a distance of 0 meter

In table IV is the result of the implementation of a built-in antenna with a 4x2 diamond patch microstrip antenna I-slot.

TABLE IV
RESULTS OF THE IMPLEMENTATION OF A BUILT-IN ANTENNA WITH A DIAMOND I-SLOT ARRAY MICROSTRIP PATCH ANTENNA 4X2

Antenna	RSSI			
	0 meter	10 meter	20 meter	30 meter
Built in USB wireless 802.11N	-49 dBm	-61 dBm	-66 dBm	-77 dBm
Antenna microstrip patch diamond I-slot array 4x2	-45 dBm	-55 dBm	-63 dBm	-72 dBm

Based on Table IV, there is an RSSI value between a standard antenna and a diamond patch microstrip antenna with an I-slot. Therefore, the power difference can be calculated using the following equation:

$$\begin{aligned} \text{Power Difference} &= \text{RSSI}_{\text{microstrip}} - \text{RSSI}_{\text{built-in}} \\ &= -55\text{dBm} - (-66\text{dBm}) \\ &= 11\text{dBm} \end{aligned} \quad (6)$$

The power received from the 802.11n usb wireless when using a 4x2 diamond i-slot array patch microstrip antenna is greater than that of a standard antenna with a difference value of 11dBm.

IV. CONCLUSION

Based on the comprehensive research and detailed testing that have been conducted, it has been determined that the microstrip patch diamond i-slot 4x2 array antenna exhibits several notable characteristics. The antenna achieved a return loss of -18.10 dBm at a frequency of 2457 MHz, coupled with a Voltage Standing Wave Ratio (VSWR) of 1.28, indicating efficient performance at this frequency. Additionally, the bandwidth measurement of the antenna revealed a value of 84 MHz, which signifies a reasonable range of frequency operation. The radiation pattern analysis further demonstrated that the antenna has a Half-Power Beamwidth (HPBW) of 52°, with a clearly defined directional radiation pattern. Moreover, the implementation of the Received Signal Strength Indicator (RSSI) showed that the microstrip patch diamond i-slot 4x2 array antenna achieved a power level that was 11 dBm higher than that of the built-in 802.11N antenna, indicating a significant improvement in performance.

REFERENCES

- [1] L. Anchidin, A. Lavric, P. M. Mutescu, A. I. Petrariu, and V. Popa, "The design and development of a microstrip antenna for Internet of Things applications," *Sensors*, vol. 23, no. 3, p. 1062, Jan. 2023.
- [2] K. N. Olan-Nuñez, R. S. Murphy-Arteaga, and E. Colín-Beltrán, "Miniature patch and slot microstrip arrays for IoT and ISM band applications," *IEEE Access*, vol. 8, pp. 102 846–102 854, 2020.
- [3] M. I. Jais, M. F. Jamlos, M. Jusoh, T. Sabapathy, M. R. Kamarudin, and A. A. A. Azremi, "A novel 2.4/5 GHz dual-band rectangular ring dielectric resonator antenna for WLAN application," *IEEE Access*, vol. 8, pp. 36099–36105, 2020.
- [4] F. Zarrabi, P. Shokri, and Z. Mansouri, "Multibranch monopole antenna with dual-band notch using U-shaped slot and butterfly shape conductor-backed plane for UWB application," *AEU - Int. J. Electron. Commun.*, vol. 113, p. 152991, Jan. 2020.
- [5] S. K. Patel and Y. P. Kosta, "Metamaterial-loaded compact high-gain dual-band rectangular microstrip patch antenna for C- and X-band applications," *Int. J. RF Microw. Comput.-Aided Eng.*, vol. 30, no. 6, e22176, Jun. 2020.
- [6] J. S. Row and S. H. Chen, "Wideband base station antenna array using coupled microstrip patch elements for sub-6 GHz 5G applications," *IEEE Trans. Antennas Propag.*, vol. 70, no. 5, pp. 3544–3552, May 2022.
- [7] M. S. Khan, A. D. Capobianco, A. Naqvi, S. Asif, D. E. Anagnostou, and B. Ijaz, "A compact, ultra-wideband antenna with triple band-notched characteristics for WLAN and WiMAX applications," *AEU - Int. J. Electron. Commun.*, vol. 117, p. 153091, Mar. 2020.
- [8] K. K. H. Li and K. M. Luk, "A wideband circularly polarized antenna with gain enhancement for 60-GHz applications," *IEEE Trans. Antennas Propag.*, vol. 69, no. 4, pp. 1975–1984, Apr. 2021.
- [9] Y. Liu, H. Zhang, L. Zhu, S. Gao, and Z. Feng, "A low-profile wideband circularly polarized patch antenna array for 5G millimeter-wave applications," *IEEE Trans. Antennas Propag.*, vol. 70, no. 3, pp. 1890–1901, Mar. 2022.
- [10] S. Verma, N. R. K. Nirala, and R. L. Yadava, "Gain and bandwidth enhancement techniques in microstrip patch antennas: A review," *Int. J. RF Microw. Comput.-Aided Eng.*, vol. 32, no. 1, e22945, Jan. 2022.
- [11] M. T. Islam, M. S. J. Singh, M. R. I. Faruque, and A. T. Mobashsher, "A compact UWB antenna with independently controllable notch bands," *Sensors*, vol. 19, no. 6, p. 1411, Mar. 2019.
- [12] M. M. M. Ali, A. R. Sebak, and A. A. Kishk, "Wideband millimeter-wave circularly polarized antenna using metasurface-inspired multiple-mode resonator," *IEEE Trans. Antennas Propag.*, vol. 69, no. 5, pp. 2564–2574, May 2021.
- [13] H. Malekpoor and S. Jam, "Bandwidth enhancement of a rectangular patch antenna using I-shaped slot for WLAN/WiMAX applications," in *Proc. 27th Iran. Conf. Elect. Eng. (ICEE)*, 2019, pp. 1729–1732.
- [14] A. A. R. Saad and D. Heberling, "Compact dual-band I-slot microstrip patch antenna for robust satellite navigation," *IEEE Antennas Wireless Propag. Lett.*, vol. 18, no. 11, pp. 2404–2408, Nov. 2019.
- [15] P. P. Shome, T. Khan, and A. K. Laha, "Design and analysis of a diamond-shaped microstrip patch antenna for ultra-wideband application," in *Proc. IEEE Indian Conf. Antennas Propag. (InCAP)*, 2019, pp. 1–4.
- [16] S. K. Jain, A. K. Yadav, and P. K. Singhal, "Performance analysis of diamond-shaped microstrip patch antenna with slots for X-band applications," *Prog. Electromagn. Res. C*, vol. 103, pp. 25–36, 2020.
- [17] Koesmarijanto, A. Azizah, and H. Darmono, "Design and implementation of 2x4 truncated corner patch microstrip antenna with U-slot at 2.4 GHz frequency for Wi-Fi applications," *J. Telecommun. Netw.*, vol. 12, no. 4, pp. 251–257, 2022.
- [18] M. I. Muttaqin, H. Darmono, and Koesmarijanto, "Design and implementation of 2x4 octagonal array patch microstrip antennas using T-slots at 2.4 GHz frequency for wifi applications," *J. Telecommun. Netw.*, vol. 13, no. 2, pp. 169–176, 2023.